

First-principles calculations of engineered surface spin structuresChiung-Yuan Lin¹ and B. A. Jones²¹*Department of Electronics Engineering and Institute of Electronics, National Chiao Tung University, Hsinchu, Taiwan*²*IBM Almaden Research Center, San Jose, California 95120-6099, USA*

(Received 2 November 2009; revised manuscript received 6 July 2010; published 18 January 2011)

The engineered spin structures recently built and measured in scanning tunneling microscope experiments are calculated using density functional theory. By determining the precise local structure around the surface impurities, we find that the Mn atoms can form molecular structures with the binding surface, behaving like surface molecular magnets. The spin structures are confirmed to be antiferromagnetic, and the exchange couplings are calculated within 8% of the experimental values simply by collinear-spin generalized gradient approximation + U calculations. We can also explain why the exchange couplings significantly change with different impurity binding sites from the determined local structure. The bond polarity is studied by calculating the atomic charges with and without the Mn adatoms. In addition, we study a second adatom, Co. We study the surface Kondo effect of Co by calculating the surrounding local density of states and the on-site Coulomb U and compare and contrast the behavior of Co and Mn. Finally, our calculations confirm that the Mn and Co spins of these structures are $5/2$ and $3/2$, respectively, as also measured indirectly by scanning tunneling microscope.

DOI: [10.1103/PhysRevB.83.014413](https://doi.org/10.1103/PhysRevB.83.014413)

PACS number(s): 75.30.Hx

I. INTRODUCTION

Assembling and manipulating a few spins (1~20) is essential for the development of nanoscale magnetic devices. During the past decades, chemists have been able to synthesize molecular magnets that carry giant molecular spins. Potential applications of molecular magnets have been extensively proposed in the literature¹ such as magnetic storage bits, quantum computation, and magneto-optical switches. The atoms within a molecular magnet form chemical bonds with each other and therefore are very difficult to manipulate. Instead of assembling atomic spins chemically to form isolated molecules, the advance of manipulating atoms on surfaces by scanning tunneling microscope (STM) has made it possible to make, probe, and manipulate individual atomic spins.

In a pioneering experiment, Hirjibehedin *et al.*² carried out low-temperature STM measurements of atomic chains of up to 10 Mn atoms. These magnetic chains are assembled by atomic manipulation on copper nitride islands that provide an insulating monolayer between the chains and a Cu(100) substrate (to be called the CuN surface later in this paper). Reference 2 shows the calculation of exchange coupling J using the Heisenberg Hamiltonian to be successful. It demonstrated that the exchange coupling J can be tuned by placing the magnetic atoms at different binding sites on the substrate. Nevertheless, the STM experiments cannot provide either a detailed study of the single CuN layer or the subatomic spatial structures around the Mn atoms. As we will show in this work, the former can explain why tunneling current and spin can both be preserved, and the latter is essential for realizing the molecular magnetism of the Mn-surface complex as well as understanding how J depends on the Mn binding site. Moreover, the $5/2$ spin of the Mn atoms on such a CuN surface is calculated directly here rather than indirectly, extracting from inelastic-tunnelling-spectroscopy steps in the experiments.

There have been a few previous reports of density functional theory (DFT) studies of this system. Shick *et al.*³ studied the magnetic anisotropy of a single Mn adatom. Recent attempts

in applying DFT to study the spin coupling in such systems have been limited to projected-augmented-wave (PAW) and pseudopotential approaches. For example, Rudenko *et al.*⁴ achieve very good agreement for the spin coupling of the Cu-site Mn atoms by using the U value from our full-potential linearized augmented plane wave (FLAPW) calculation (done as groundwork for the results presented in this paper). Scopel *et al.*⁵ study the ratio of the spin couplings between the Cu and N sites but use only $U = 0$ and, as a result, do not obtain very good agreement with experiments. In fact, these methods do not have the ability to calculate the U value and always need either to take U from an FLAPW DFT or to treat U as a parameter fitted to the experiments.

In addition to the interatomic magnetic coupling, the surface Kondo effect is also an interesting topic in engineered spin systems. Recent studies show that the surface Kondo effect is interestingly influenced by either the magnetic anisotropy of the Kondo atom itself⁶ or by being coupled to a second magnetic atom.⁷ These systems both have Co as the adatom for their Kondo impurity and are built on the CuN surface that was previously used to study coupling of Mn atoms. These experimental studies explain surface Kondo under external influences using phenomenological models and obtain great success. However, detailed microscopic understanding such as the local density of states (LDOS) around the Co and the on-site Coulomb repulsion U were not achieved yet. Also, Ref. 4 concludes indirectly that the Co spin on this surface is $S = 3/2$ by first excluding $S = 1/2$ and integer S from the experimental fitting and then excluding $S \geq 5/2$ based on the experience that the spins of surface-adsorbed atoms are generally unchanged or reduced from the free atom. Yet a direct measurement or calculation was not done.

In this paper, we perform first-principles calculations of the clean CuN surface and of Mn and Co adatoms on this surface with structure optimization. We find, surprisingly, that when the Mn atoms are deposited on the Cu sites of the CuN surface, the nearby N atoms break bonds with their neighboring Cu and form a quasi-molecular structure on the surface, a situation that does not happen for Mn at the N sites. This fact itself was

not determined from experiment and can only be realized from a first-principles calculation. As a comparison, we study the clean CuN surface and find that the CuN monolayer is formed by polar covalently bounded Cu and N, and such a layer is shown to provide a semimetal surface layer on the underlying Cu substrate, allowing the coexistence of the Mn spin and STM current. We also accurately calculate the exchange coupling J using the generalized gradient approximation (GGA) + U method, from which we demonstrate that first-principles calculation has the capability of predicting J of given physical systems. For a Co atom on the same surface, we determine the on-site Coulomb U that is very important in understanding the Kondo effect. We also compare the LDOS of Co on the Cu and N sites and explain why the Kondo effect is observed in the experiments on the Cu site but not on the N. Finally, we determine, by analyzing the Co density of states, a Co spin that matches what was measured indirectly from STM experiments.⁶

II. THEORY

The CuN monolayer between the magnetic atoms and Cu substrate originates from the idea of preserving the atomic spins from being screened by the underlying conduction electrons, while at the same time allowing enough tunneling current from a STM tip to probe the spin excitations. To understand this further in a microscopic picture, we simulate both the Cu(100) and CuN surfaces by a supercell of slabs separated by eight vacuum layers, where for the CuN surface, each slab has CuN monolayers on both sides and three Cu layers in between. The thickness of a slab was taken to be five, seven, and nine layers of Cu, and by calculation of atomic positions and electronic properties, we found that the five-layer slab is already adequate to obtain precise positions of N and the surface Cu. The electronic structure is calculated, in the framework of density functional theory, using the all-electron FLAPW method⁸ with the exchange-correlation potential in GGA.⁹ We calculate the LDOS of both the Cu(100) and CuN surfaces at the Fermi energy along the z direction, perpendicular to the surface, through the surface Cu atom. As seen from Fig. 1, the LDOS of the clean Cu(100) surface

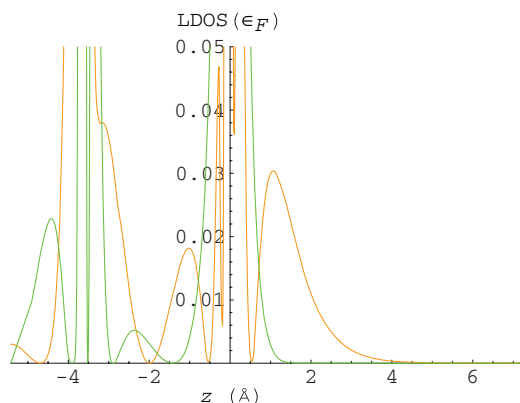


FIG. 1. (Color) LDOS(ϵ_F) along the out-of-surface direction with the surface Cu atom as the origin, for both the clean Cu(100) (orange) and CuN (green) surfaces. (The vacuum corresponds to positive values of z .)

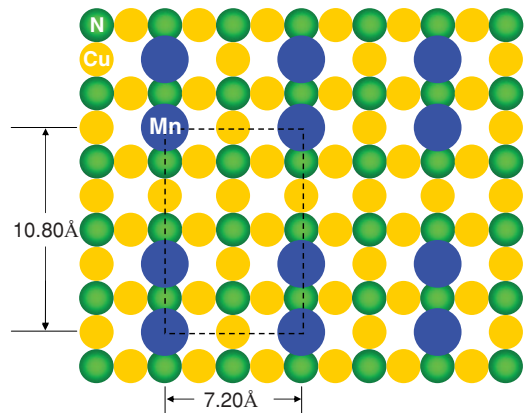


FIG. 2. (Color online) Unit cell of a Mn dimer on the CuN surface.

has a much longer tail into vacuum than the CuN surface. The calculated work functions are 4.6 and 5.2 eV, respectively, a difference of 0.6 eV, much smaller than a typical bulk insulator, which has a work function $\gtrsim 3$ eV more than copper. This shows that the CuN monolayer provides the Cu substrate a moderate conduction that makes possible the coexistence of the atomic spin and STM current.

To calculate the electronic structures of Mn(Co) on the CuN surface, we simulate the single magnetic atom on this surface by a supercell of five-layer slabs similar to the one for the CuN surface with the Mn(Co) atoms placed on top of the CuN surface at 7.24 Å separation. The crystal structure is optimized until the maximum force among all the atoms reduces to $\lesssim 2$ mRy/ a_0 . The $3d$ orbital can in general have strong Coulomb repulsion U that cannot be taken into account by GGA. Using a constraint-GGA method,¹⁰ we obtain the U value of a single Mn at the Cu site of the CuN surface to be 4.9 eV, and 3.9 eV at the N site. Since the calculated Mn U s fall in the range of strong correlation, they are then used in the GGA + U calculation^{11,12} for Mn $3d$. To calculate a Mn dimer on the CuN surface, we simulate the system using the same slab setup as for the single Mn, except that the Mn atoms on the surface are arranged as in Fig. 2. The electronic structure is also calculated using GGA + U with U on the Mn $3d$ orbitals. For Co on the Cu site, we also apply the constraint-GGA method and obtain $U = 0.8$ eV. We then calculate this system by GGA with no additional U . In fact, since the experiments show that such a Co adatom exhibits the Kondo effect, it does not make sense to apply the U statically in a dynamical process (Kondo).

III. RESULTS AND DISCUSSION

To see the effect on the surface of the presence of Mn atoms, and to form a background for our work, we replot in Fig. 3 our electron density of the clean CuN surface that previously appeared, and was briefly discussed, in a paper addressing the magnetic anisotropy of a single Fe adatom.¹³ We find the N atoms snug in between the surface Cu atoms to form a CuN surface layer, joined by shared charge densities as well as proximity. The vertical distance between N and the surface Cu is only 0.26 Å, essentially collinear. The density contour shared by N and Cu indicates that a polar



FIG. 3. (Color online) Electron density contour of the CuN surface along the N row and the out-of-plane directions.

covalent bond is formed between Cu (metallic) to N (larger electronegativity). In fact, a Bader analysis¹⁴ on our calculated electron-density distribution shows that N and surface Cu are -1.2 and $+0.6$ charged, respectively. Figure 4 (a version of which also previously appeared in Ref. 13) shows the electron density contour of a single Mn atom placed on the Cu atom on this surface. As one can see, the atomic structure is substantially rearranged. The Mn atom, sitting 1.6 Å atop the surface, attracts its neighboring N atoms remarkably out of the surface by 0.8 Å, forming a new polar covalent bond that replaces the CuN binding network, and the Cu atom underneath Mn moves 0.8 Å toward the bulk. We have calculated that Mn and its neighboring N are $+1.0$ and -1.3 charged, respectively, indicating that the Mn-N bond has a stronger polarity than the Cu-N bond.

The calculated density of states for a single Mn on the CuN surface is plotted in Fig. 5. It is clearly seen that the Mn $3d$ majority spin states are all below the Fermi level and the minority states are all above, which implies a $3d^5$ configuration for Mn, a spin $S = 5/2$ configuration. We also do the same analysis for Mn at the N site of the CuN surface, and this structure exhibits the same unchanged Mn spin. This verifies the same conclusion drawn from comparing spin chains of different lengths in the STM experiment.² The

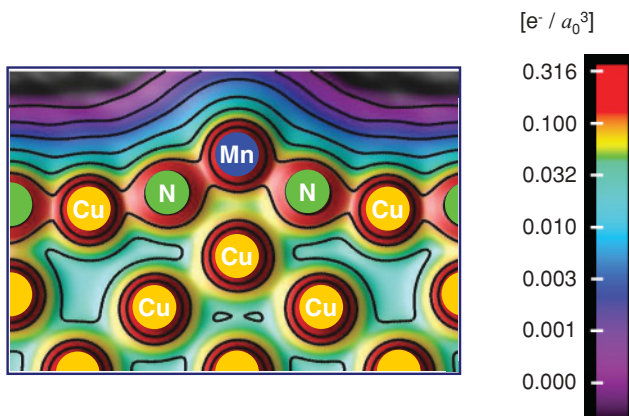


FIG. 4. (Color online) Electron density contour of a single Mn on the CuN surface along the N-Mn-N row and the out-of-plane directions.

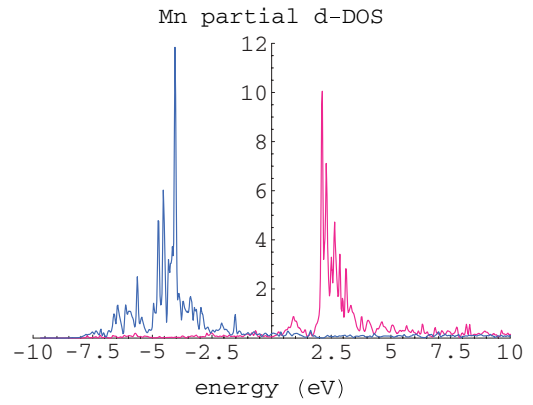


FIG. 5. (Color online) Mn d -projected density of states of a single Mn on the CuN surface [the leftmost curve (blue in color) for spin-up and the rightmost curve (pink) for spin-down].

Mn $+1.0$ charge and $5/2$ spin are seemingly inconsistent to each other if one utilizes the free-atom picture to conclude a valance configuration $3d^5 4s^1$ for the former and $3d^5$ for the latter. This conceptual problem can be explained as follows. The key point is to notice that charges are calculated in a Bader's atomic basin, which is a region slightly different from where the atomic DOS is defined: the muffin-tin sphere. Since the DOS analysis exhibits a half-filled $3d$ shell, the lost electron of Mn cannot come from $3d$ but only from $4s$. As we also analyzed, the $4s$ character is absent from the DOS within the Mn muffin-tin sphere. This means that one $4s$ electron contributes the polar covalent bond between Mn and N by primarily occupying the interstitial region (outside the Mn muffin-tin sphere but still being included by Mn Bader analysis), and the other $4s$ electron undergoes charge transfer to the neighboring N (not included by Mn Bader analysis). We now consider the exchange coupling of a dimer of Mn. The spin excitation measured by STM² occurs between the antisymmetric spin ground state and the first excited state. These quantum atomic-spin states are not accessible by density-functional electronic-structure calculation. However, the collinear spin states (with parallel and antiparallel spins) of a Heisenberg spin dimer exactly correspond to the collinear magnetic-moment configurations of the real crystal system of the Mn dimer absorbed on the CuN substrate. The parallel and antiparallel spin states have energy expectation values $\pm JS^2$, respectively. One simply takes the difference of the total energies between parallel and antiparallel-spin configurations of the dimer on the CuN surface and then extracts J from this energy difference δE and S by the following equation:

$$\delta E = JS^2 - (-JS^2) = 2JS^2. \quad (1)$$

The actual computation of total energies of the Mn dimer on CuN is done by controlling the number of plane waves with $R_{\text{MT}_{\min}} K_{\text{max}}$ times K_{max} , where $R_{\text{MT}_{\min}}$ is the muffin-tin sphere of the smallest atom (N in this case) and K_{max} is the plane-wave cutoff. We have used $R_{\text{MT}_{\min}} K_{\text{max}} = 5.6 \sim 6.2$ and observed the convergency of the J values with respect to $R_{\text{MT}_{\min}} K_{\text{max}}$. For a Mn dimer at the Cu site of a CuN surface, we obtain an exchange coupling of $J = 6.4$ meV from Eq. (1), which shows excellent agreement with the STM-measured $J = 6.2 \pm 0.2$ meV. In order to show that this agreement is

TABLE I. Different calculations of exchange coupling J (in meV) of Mn dimers on the CuN surface, compared with the experiments, where the present work adopts GGA + U LAPW.

	Cu site	N site
LDA + U PAW ⁴	6.8	(not calculated)
LDA + U TB-LMTO-ASA ⁴	6.5	(not calculated)
GGA pseudopotential ⁵	~13	~6
GGA + U LAPW	6.5	2.5
STM ²	6.2	2.7

not just a coincidence, we do the same calculation for a Mn dimer on the N site. The exchange coupling J turns out to be 2.5 meV, which is also close to the STM measurement ($J = 2.7$ meV) and is roughly half of the Cu-site J .

We also compare our results with previous calculations of J , as in Table I. One can see that inclusion of Coulomb on-site U substantially improves the J values and agrees very well with the experiments. It is also worth mentioning that PAW and TB-LMTO-ASA methods are not capable of calculating the U values but need to take U from our constraint-GGA calculation in the FLAPW basis.⁴ Thus we have demonstrated that the FLAPW GGA + U method reproduces the exchange coupling between these engineered spins and will have the capability of predicting similar systems.

In order to check whether it is reasonable to use the U values determined by the constraint-GGA method in calculating J , we also calculate J using other U values. The resulting J s are listed in Table II. We note the significant lack of agreement with experimental values of J using alternative U s. This strongly suggests that the constraint-GGA method of obtaining U is likely to be a quite reliable predictor of the exchange couplings of similar spin systems.

The electron density contour of the N-site Mn dimer shows a structure completely different from Mn on the Cu site, as shown in Fig. 6. The Mn dimer on the Cu site forms a chainlike structure bridged by the significantly lifted middle N atom, while on the N site, the Mn is attached to the surface like a crown. The binding structures of the Mn atoms strongly suggest that the Mn spins are coupled through the N atoms. The electron density contours indicate that the Mn dimer at the Cu site has a coupling path considerably shorter than when in the surprisingly different structure at the N site. We propose that this explains why the exchange coupling J measured by STM for the Cu-site Mn dimer has a value twice that of the N site.

Co atoms on the CuN surface behave quite differently from Mn, as experiments^{6,7} show. Co displays a Kondo effect, while

TABLE II. Calculated exchange coupling J (in meV) of Mn dimers on the CuN surface at different U values.

	Cu site	N site
GGA	18.5	-1.8
GGA + U (calculated U)	6.50 ± 0.05 ($U = 4.9$ eV)	2.5 ($U = 3.9$ eV)
GGA + U (calculated $U + 1$ eV)	5.4	5.1

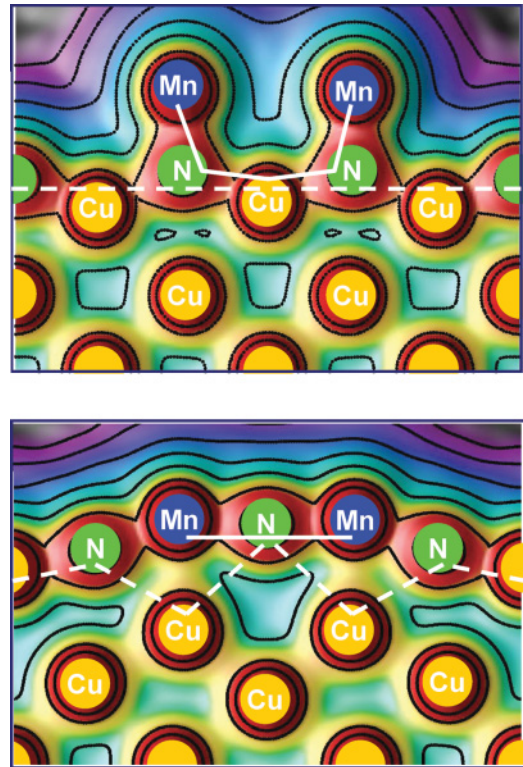


FIG. 6. (Color online) Electron density contours of Mn dimers at the (top) N and (bottom) Cu sites of the CuN surface along the dimer row and the out-of-plane directions. The white solid lines show our proposed coupling path between Mn spins. The dashed lines show how corrugated the clean CuN surface becomes in the presence of Mn adatoms. The contour scales are identical to Fig. 4.

Mn does not. The relaxed structure via our calculation is shown in the electron-density contour plotted in Fig. 7. As one can see, the Co atom, sitting 1.7 Å atop the surface, attracts its neighboring N atoms out of the surface by 0.7 Å, and the Cu atom underneath Co moves 0.5 Å toward the bulk. Co settles closer to the underneath Cu than Mn does and so interacts more with the conduction electrons. We also compare the surface

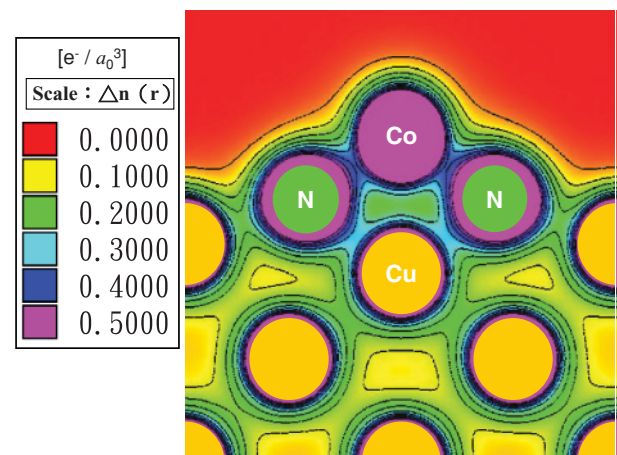


FIG. 7. (Color online) Electron density contour of a single Co on the CuN surface along the N-Co-N row and the out-of-plane directions.

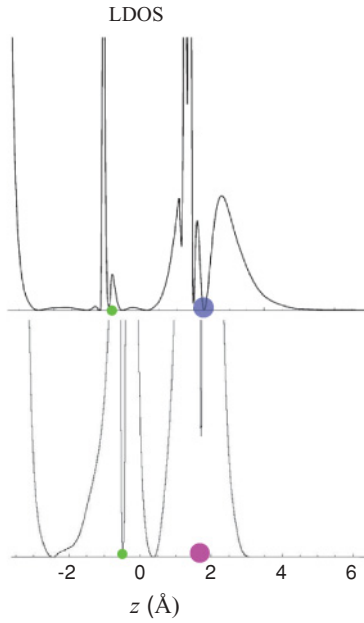


FIG. 8. (Color online) LDOS(ϵ_F) along the out-of-surface direction through the adatoms Mn (the larger, solid blue circle in the upper plot) and Co (the larger, solid purple circle in the lower plot) on the CuN surfaces. The smaller, solid green circles are the Cu atoms underneath the adatoms. The origin is chosen at location of the surface Cu atom of the clean CuN surface, and the vacuum corresponds to positive values of z .

LDOS with Co and Mn, as in Fig. 8, and find that there is more LDOS between Co and the Cu underneath it than for Mn. This fact can also be seen by comparing the charge contour plots of these two systems (see Figs. 4 and 7). Such substantial LDOS near Co provides the conduction electrons needed for a Kondo effect to happen.

To find the Co spin from our calculation, we plot the densities of states of the $3d$ Co on the CuN surface, as in Fig. 9. One clearly sees that the spin-up total density of states and the spin-down $3d_{x^2-y^2}$ and $3d_{yz}$ ones are all occupied, while the rest are majority unoccupied. Additionally, we also

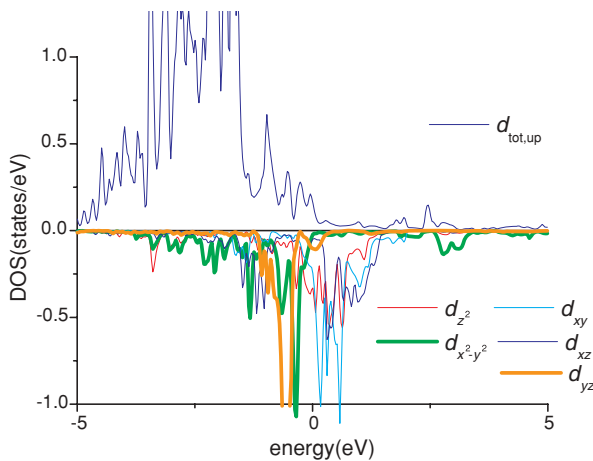


FIG. 9. (Color online) The Co $3d$ densities of states on the CuN surface. Positive (negative) refers to spin-up (spin-down).

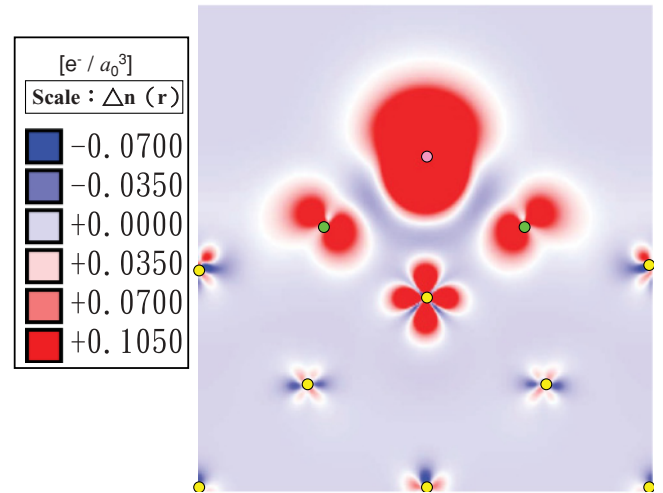


FIG. 10. (Color online) Spin density contour of a single Co on the CuN surface along the N-Co-N row and the out-of-plane directions. Pink, green, and yellow solid circles denote Co, N, and Cu atoms, respectively.

check that the $4s$ character is indeed absent from the DOS. This density-of-state analysis gives $S = 3/2$ for Co on the CuN surface by approximating the Co $3d$ in terms of an atomlike electron configuration of five spin-up and two spin-down electrons. The charge of Co calculated by Bader analysis is $+0.8$, which has a free-atom valance configuration $3d^7 4s^1$ that is seemingly inconsistent with the $4s$ -absent $S=3/2$ free atom $3d^7$. The situation is basically the same as that of Mn, as explained in the previous paragraph.

Another interesting point is to compare the U values of Co on Au(111) and this CuN/Cu(100) surface since Co/Au(111)¹⁵ is one of the most extensively studied surface Kondo systems. The on-site Coulomb repulsion of Co on Au(111) was extracted to be 2.8 eV from a previous first-principles calculation.¹⁶ The present study has obtained $U = 0.8$ eV for Co on the CuN surface. The substantial difference of Co U of the two systems can be explained in the way that Co surrounded by N is more positively charged than that on Au(111), so adding an electron into Co on CuN is easier because a Co ion attracts an electron more strongly.

Finally, we calculate the spin polarization of Co on the CuN/Cu(110) surface, shown in Fig. 10. We see the strong spin coupling of the Co, not only to the N on either side, but also to the Cu underneath. In addition, a Co-generated spin polarization is evident in all of the other Cu in the system as well, confirming the availability of Cu for a Kondo effect of the Co.

IV. CONCLUSIONS

In summary, we have calculated the electronic structures of newly engineered spin systems. The precise atomic charges and positions of those systems, not accessible by experimental techniques, are determined by structure relaxation and Bader analysis, respectively, in our calculations. The charge analysis shows that the Mn-N bond formed by Mn adsorbed on the CuN surface has stronger bond polarity than the Cu-N bond. The presence of Mn gives rise to substantial rearrangement

of the atomic structure: The Mn atoms at the Cu sites perturb their surrounding atomic positions, while those at the N sites do not. The calculated J s agree excellently with the STM measurements for two different Mn binding sites, without treating the U value in a GGA + U (or LDA + U) approach as a fitting parameter. Such agreement serves as a touchstone of DFT's future predictability in similar systems and is important in searching for a desired J (e.g., large value or ferromagnetic) for device applications, with the goal of avoiding multiple experimental trials.

The electronic and spin structure of Co atoms on the same surface is also calculated. From that, we explain why Co has a Kondo effect, while Mn does not. We also find the Co spin to be $S = 3/2$, in agreement with the STM's indirect derivation.⁶

The on-site Coulomb repulsion is calculated to be $U = 0.8$ eV, much smaller than that of the popular surface Kondo system Co/Au(111), which we explain by the polarities of Co to its nearest-neighbor atoms.

ACKNOWLEDGMENTS

We thank C. F. Hirjibehedin, C. P. Lutz, and A. J. Heinrich for stimulating discussions and the technical help of the IBM Almaden Blue Gene support team. C.-Y.L. acknowledges support from the Taiwan National Science Foundation, the Taiwan National Center for High-Performance Computing, and the Taiwan National Center for Theoretical Sciences (South).

¹B. Barbara and L. Gunther, *Phys. World* **12**, 35 (1999); D. Gatteschi and R. Sessoli, *Angew. Chem. Int. Ed.* **42**, 268 (2003); M. Verdager, *Polyhedron* **20**, 1115 (2001).

²C. F. Hirjibehedin, C. P. Lutz, and A. J. Heinrich, *Science* **312**, 1021 (2006).

³A. B. Shick, F. Maca, and A. I. Lichtenstein, *Phys. Rev. B* **79**, 172409 (2009).

⁴Some of the results of our work were previously presented at the APS March meeting 2006 and was cited by A. N. Rudenko, V. V. Mazurenko, V. I. Anisimov, and A. I. Lichtenstein, *Phys. Rev. B* **79**, 144418 (2009). This paper is then cited by a similar work.⁵

⁵W. L. Scopel, P. Venezuela, and R. B. Muniz, *Phys. Rev. B* **79**, 132403 (2009).

⁶A. F. Otte *et al.*, *Nat. Phys.* **4**, 847 (2008).

⁷A. F. Otte *et al.*, *Phys. Rev. Lett.* **103**, 107203 (2009).

⁸P. Blaha *et al.*, computer code **WIEN2k**: An Augmented Plane Wave plus Local Orbitals Program for Calculating Crystal

Properties, Vienna University of Technology, Vienna, Austria, 2001.

⁹J. P. Perdew, K. Burke, and M. Ernzerhof, *Phys. Rev. Lett.* **77**, 3865 (1996).

¹⁰G. K. H. Madsen and P. Novák, *Europhys. Lett.* **69**, 777 (2005).

¹¹V. I. Anisimov, I. V. Solovyev, M. A. Korotin, M. T. Czyzyk, and G. A. Sawatzky, *Phys. Rev. B* **48**, 16929 (1993).

¹²A. I. Liechtenstein, V. I. Anisimov, and J. Zaanen, *Phys. Rev. B* **52**, R5467 (1995).

¹³C. F. Hirjibehedin, C. Y. Lin, A. F. Otte, M. Ternes, C. P. Lutz, B. A. Jones, and A. J. Heinrich, *Science* **317**, 1199 (2007).

¹⁴R. F. W. Bader, *Atoms in Molecules: A Quantum Theory* (Clarendon, Oxford, 1990).

¹⁵V. Madhavan, W. Chen, T. Jamneala, M. F. Crommie, and N. S. Wingreen, *Science* **280**, 567 (1998).

¹⁶O. Újsághy, J. Kroha, L. Szunyogh, and A. Zawadowski, *Phys. Rev. Lett.* **85**, 2557 (2000).